Towards realistic COOLFluiD global coronal model for EUHFORIA 2.0 space weather forecast: magnetograms reconstruction and comparison with observations.

Błażej Kuźma
Center for mathematical Plasma Astrophysics, Department of Mathematics, KU Leuven, Belgium

Michaela Brchnelova[1], Barbara Perri[1], Tinatin Baratashvili[1], Fan Zhang[1], Andrea Lani[1], Stefaan Poedts[1,2]
[1]Center for mathematical Plasma Astrophysics, Department of Mathematics, KU Leuven, Belgium
[2]Institute of Physics, University of Maria Curie-Skłodowska, Poland

ABSTRACT

We developed COolfluid COroNa UnsTructured (COCONUT) - a novel global coronal model based on the COOLFluiD numerical code. The steady-state solution is determined by the inner boundary defined by magnetogram data in combination with fixed hydrodynamic values representative of the typical corona, while inside the numerical domain of our simulation, the corona is described by the set of ideal-MHD equations with gravity. The latter is solved with use of an implicit solver on an unstructured grid. Our code has passed a set of benchmark tests and proved its accuracy for simple dipole / quadrupole solutions as well as for a wide range of magnetograms, both during solar minima and solar maxima. With various numerical optimization techniques and an adaptive CFL step, we decreased the computation time while maintaining the high robustness and reliability. Finally, we coupled the obtained results with the heliospheric wind model of EUHFORIA 2.0 space weather forecast to show its forecast abilities. All this leads to an accurate MHD solution obtained within only a few hours of computation, which is crucial for space weather forecast systems.

Here we present some of the numerically obtained results for selected magnetograms chosen to represent a variety of stages of the solar activity, from minimum to maximum, with each of them corresponding to a particular solar eclipse, to allow us the direct comparison of simulations with the observed coronal structures. Following the commonly used procedure, the input raw / original MDI and HMI magnetograms are pre-processed by projection on spherical harmonics and a selection of a maximum frequency for the reconstruction. This is equivalent to a smoothing of the map and results in removal of the small, intense magnetic structures on the solar surface. These are in fact numerically more challenging to capture, while their contribution to the overall structure of the solar wind at 0.1 AU and the large-scale coronal magnetic fields has not been thoroughly investigated yet. With several maps and several levels of accuracy of reconstruction we address this problem and show the map resolution and pre-processing impact on accuracy of the numerical results. This is especially important for computationally challenging maximum-activity magnetograms which require significant pre-processing for stability and satisfactory computational speed.

To verify our numerical results, we use a validation scheme proposed by Wagner et al. 2022 (from less to more sophisticated methods, i.e., visual classification, feature matching, streamer direction and width, brute force matching, topology classification). We investigate the distribution of magnetic structures as predicted by our simulations and compare them to the obtained coronal magnetic field topology. The detailed comparison with observations reveals that our model recreates relevant features such as the position and the shape of the streamers (by comparison with white-light images), the coronal holes (by comparison with EUV images) and the current sheet (by comparison with WSA model at 0.1 AU). We conclude that an unprecedented combination of accuracy, computation speed and robustness is accomplished at this stage, with possible improvements in the foreseeable future, such as inclusion of more physics or implementation of the adaptive mesh refinement technique. Our results also show that the final solution is still very sensitive to the map chosen and its pre-processing, especially for solar maximum-activity cases

INTRODUCTION

A model of the solar corona that would allow one to obtain quick and reliable results is now one of the primary goals of space weather research [1]. This is largely motivated by our increasing dependency on space infrastructure, which is highly sensitive to solar weather. Apart from space infrastructure however, geomagnetic storms can also disrupt airborne and ground systems such as aircraft and power grids. Solar flares and other eruptive events may trigger coronal mass ejections that could potentially reach Earth in just a few days. In practice, this fact sets the time-constraints on our modelling methods and heavily limits the complexity of the models that can be utilized for space weather forecasting at 1 AU, which is the reason why (semi)empirical models such as WSA are still used nowadays.

While the computational time-constraint is definitely one of the most important factors in space weather forecasting, another such factor is also the solution accuracy [2]. This depends on how the physics of the model is treated, for example through inclusion of non-ideal terms or multiple species, but also on numerical and data-processing techniques, such as magnetogram pre-processing techniques, limiters, and numerical schemes. Without significantly increasing the computational time, on unstructured grids, better accuracy can be also obtained via techniques such as higher-order reconstruction or adaptive grid refinement. So far however, the majority of the state-of-art global coronal models work with structured grids only, which is the reason why the unstructured-grid-based COCONUT solver has been developed. In fact, many of the afore-mentioned performance-enhancement techniques are currently already in the process of being implemented and tested.

NUMERICAL MODEL OF THE SOLAR CORONA

Our global coronal COCONUT model is primarily based on the COOLFluiD (Computational Object-Oriented Libraries for Fluid Dynamics) code. It was described in great detail by Perri et al. [4] and passed a number of validation tests ranging from a simple dipole to real magnetograms. This model is based on a finite-volume, implicit backward Euler scheme contained within the COOLFLuiD platform, developed as part of a broader heliospheric model of EUHFORIA 2.0 [5], replacing the formerly used empirical WSA model. COCONUT solves for a steady-state solution through pseudo-time stepping, which means that it can take the full advantage of its implicit scheme, using CFL numbers of up to hundreds or thousands, depending on the case simulated. Within its framework we solve the following set of the ideal MHD equations in conservation form and in 3D Cartesian coordinates:

$$\frac{\partial}{\partial t}\begin{pmatrix}\rho\\ \rho\vec{v}\\ \vec{B}\\ E\end{pmatrix}+\vec{\nabla}\cdot\begin{pmatrix}\rho\vec{v}\\ \rho\vec{v}\vec{v}+\boldsymbol{I}\left(p+\frac{1}{2}|\vec{B}|^2\right)-\vec{B}\vec{B}\\ \vec{v}\vec{B}-\vec{B}\vec{v}+\boldsymbol{I}\phi\\ \left(E+p+\frac{1}{2}|\vec{B}|^2\right)\vec{v}-\vec{B}(\vec{v}\cdot\vec{B})\end{pmatrix}=\begin{pmatrix}0\\ \rho\boldsymbol{g}\\ 0\\ \rho\boldsymbol{g}\cdot\boldsymbol{u}\end{pmatrix}. \tag{1}$$

Here, ρ is mass density, p thermal gas pressure, $g(r)=-\left(GM_{\odot}/r^2\right)e_r$ gravitational acceleration, and I corresponds to the identity dyadic. We use Artificial Compressibility Analogy for divergence cleaning: $\frac{\partial\phi}{\partial t}+\mathrm{V}_{\mathrm{ref}}^2\cdot\mathrm{B}=0$. In our simulations we use unstructured 6th-level subdivided geodesic polyhedron mesh extended from 1 to 21.5 solar radii. The unstructured nature of this grid allows us to simulate polar regions with more accuracy and avoid polar degeneracy of regular grids. Compared to structured grids, it also allows for a more uniform distribution of mesh cell sizes. Our tests revealed that mesh with 1.9M elements is sufficient to recreate coronal features with sufficient level of accuracy in all discussed cases. We also use novel treatment of the inner boundary condition which, along with other techniques, reduce artificial electric field generation since it was, in the case of our solver, found to generate unphysical profiles and increase numerical dissipation [6]. On the inner boundary, aside from the magnetic field, we prescribe fixed hydrodynamic values of density and pressure representative of the typical corona along with a small velocity outflow. This outflow has its value equivalent to the Parker's solution and its magnitude aligned with the local magnetic field such that the afore-mentioned artificial generation of the corresponding electric field is limited. On the outer

supersonic boundary, we extrapolate the hydrodynamic variables and let the radial magnetic field decrease with a square of the distance. In addition, to decrease the effects caused by a potentially locally inaccurate formulation of the extrapolation laws in some regions (e.g., the center of streamers), we adjusted the mesh to have a small outer ghost cell size, which in turn limits the extrapolation distance and thus the extrapolation error.

The convergence state of the code is evaluated by computing the residual between the subsequent iterations of the implicit solver, where this residual is expressed as the logarithm of the total difference between the states of the cells in the domain. In general, to ensure complete convergence, the residuals of roughly -10 are required. However, for operational purposes where convergence times are of essence, it has been shown that to ensure sufficient convergence, residuals in velocity of -3 to -4 can be used. Finally, in some cases, especially with magnetogram-driven simulations, lower residuals cannot even be achieved due to intrinsically physically unstable current-sheets present in the solution.

As mentioned above, the obtained steady-state solution is based on the selected magnetic map used as an inner boundary condition. The pre-processing of magnetogram for this purpose will be discussed in the following section.

MAGNETIC MAPS

The COCONUT global coronal model is data-driven in the sense that we use pre-processed photospheric magnetic maps as input to be prescribed on the inner boundary. Figure 1. illustrates the study of the map reconstruction, the test-case of 1995 map (Carrington Rotation 1902). The raw magnetogram (top left panel) is pre-processed to obtain the inner boundary **Br** profile for the COCONUT run. The radial component of the raw magnetogram is projected on spherical harmonics. As we can choose different values of the maximum frequency for the latter, we ultimately obtain different levels of accuracy, with strong, intense, but small magnetic structures filtered off. Here we present the reconstructed magnetic maps for l_{max} =10, 15, 20, 25 and 30 (from top-middle panel to bottom-right). The two most distinct differences between magnetic maps with different values of l_{max}, are a) minimum and maximum values of the magnetic field strength, and b) size of the smallest magnetic structures recreated. As the magnetic field of small intense structures is smoothed, the maxima of the reconstructed magnetic field are of orders of magnitude smaller than the original photospheric magnetic field. Note that in their original shape, these small, highly intense regions would not

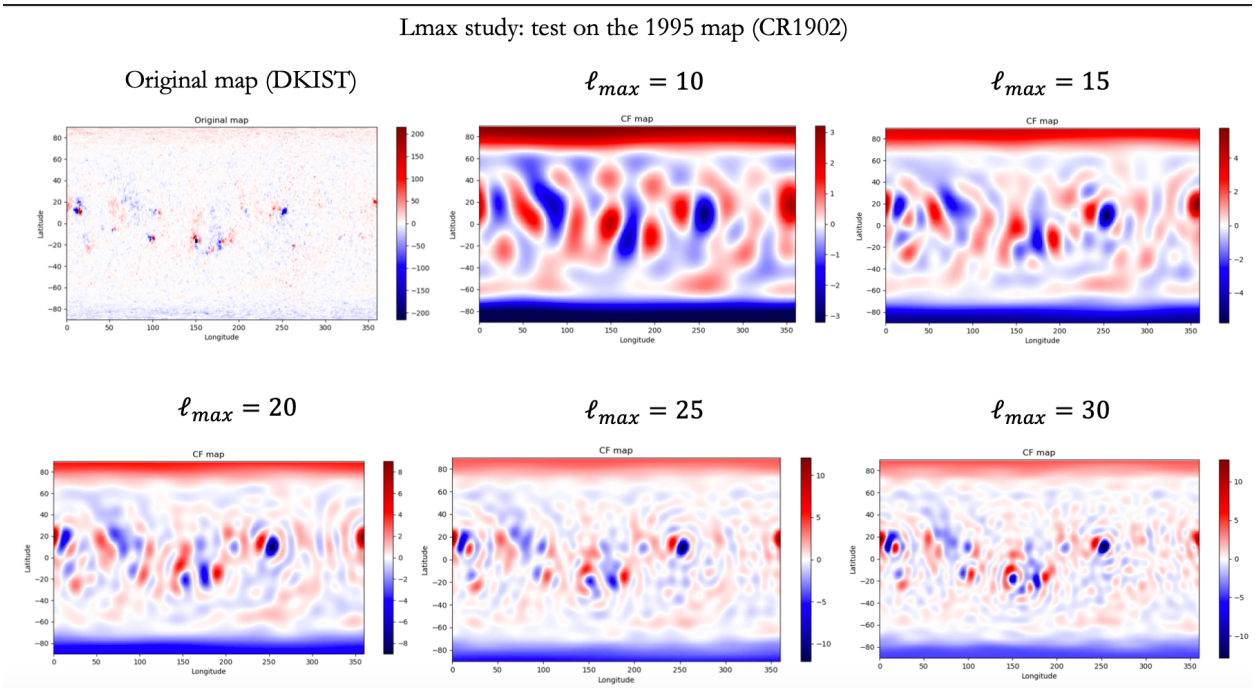

Figure 1. Magnetic map pre-processing with original magnetogram and five levels of reconstruction, from lmax=10 to 30 (from top left to bottom right).

even be properly captured due to them being smaller than surface cell size. In case they were captured, they would immediately lead to the divergence of the solver due to the very strong gradients that they would induce.

Note that the inner boundary of our simulation is placed in the solar corona, where the typical strength of the magnetic field (from 1.05 to 1.35 solar radii) is between 1 and 4 Gauss [7]. This implies that the magnitude-decreasing effect of map pre-processing is a highly desired one, as the original magnetic field of strength above 200 Gauss (Fig. 1, top left panel) would not be present in the low solar corona. Now we have to determine to what extent different levels of reconstruction affects the global results. Figure 2. illustrates how small magnetic structures (top right panel) are recreated within the inner boundary of the numerical domain (bottom right panel). We can see that even for lmax=50 the 6-th level, 1.9 M elements mesh is enough to correctly resolve fine magnetic structures.

It is expected that the increase of precision of magnetograms reconstruction (marked here with increased value of l_{max}) will mostly affect small-scale structures within active and polar regions. The first appears due to increased structure complexity, while the latter is a separate problem, with non-sufficient coverage of the polar regions by observational data. Thus the reasonable estimation of polar magnetic field has to be provided i.e. by fitting methods. In fact Figure 3 illustrates this case. We can compare here coronal structures as seen in the radial component of the plasma velocity. The largest difference between l_{max}=10, l_{max}=20 and l_{max}=30 are located either above poles or active regions, where small-scale streamers are present for l_{max}=30. However, this difference is not seen on a global scale, at the outer boundary velocities between these cases differ by no more than 10%, and this happens only above the active regions. We hence conclude that for space-weather forecast purposes, the magnetic maps with moderate levels of reconstruction are fully sufficient. In case studies more elaborate than the general space-weather forecasting are required, e.g. focusing on the dynamics and evolution of separate structures, higher resolution might be needed.

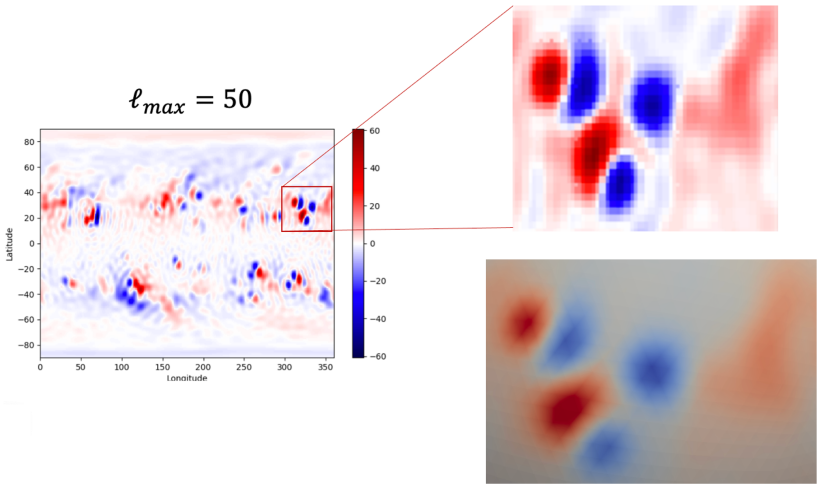

Figure 2. Projection of the small-scale features of the original magnetic map (left, top right) on the inner boundary surface (bottom right).

It is important to mention one potential issue with unprocessed maps for the case of solar maximum. The initial magnetic field can locally reach very large values, exciding 500G contained in very small areas. This leads to extreme gradients between two adjacent cells, negative temperature, and unphysical high-speed streams above. One way of fixing this issue is to limit original map min and max Br values as an additional step, before projecting it on spherical harmonics. However, this may lead to a shift in relative value of magnetic field of active regions to that of quiet Sun, affecting the alignment of streamers by a few degrees.

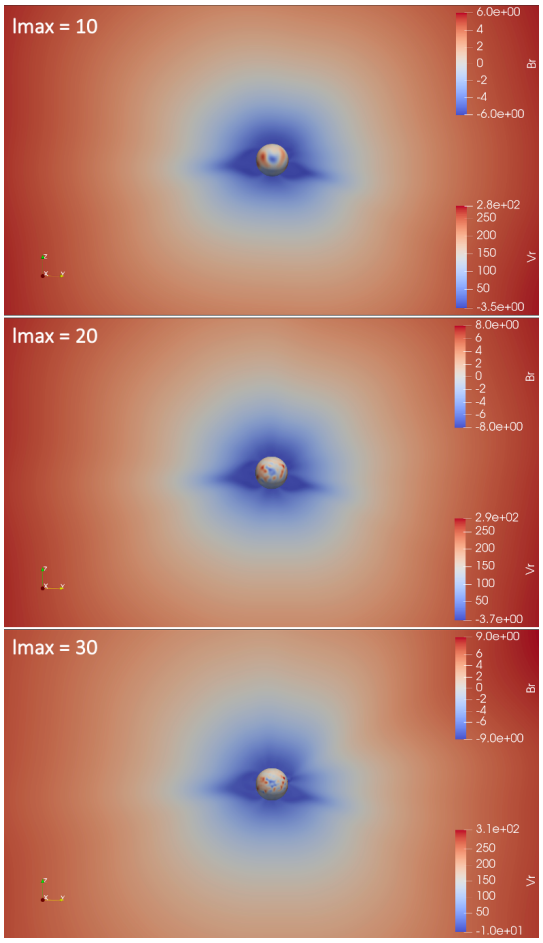

Figure 3. Impact of the map reconstruction level on the corona, the case of 2015 solar maximum. The surface colormap represents the radial magnetic field, Br, while the background colormap shows the radial velocity, Vr.

COMPARISON WITH OBSERVATIONS

Now we can move to the ultimate test every numerical code has to pass – comparison of numerically obtained results with observations, either spaceborne or in situ. For this purpose, we have chosen magnetograms corresponding to the time of the solar eclipse. This approach allows us to compare the corresponding coronal features between our simulations and those observed during the eclipse. Here we use the validation scheme of Wagner et al. [8] focusing on comparison of magnetic structures as seen within simulation in the form of magnetic field lines, with coronal structures as seen in white light image of the solar eclipse. This scheme consists of five following steps.

1) Visual classification – the idea behind this preliminary is to discard any obviously erroneous results, where there are no structures, or the one present could not be directly compared.
2) Feature matching – in this step we compare the presence, number and size of streamers and pseudostreamers extending from the solar limb.
3) Streamer direction and width – here we compare visual features of magnetic structures seen in simulations and observations.
4) Brute force matching – the step that consists of marking of distinct points (i.e. apex of the streamer seen in simulated magnetic field lines and visible apex of the streamer) and comparing their position afterwards.
5) Topology classification – here we compare the shape and size of coronal holes and regions of closed field lines seen in numerical results and observations.

Figure 4. illustrates the comparison of the actual image of the 2008 solar eclipse (left panel) with numerically obtained COCONUT data. The right panel consists of the eclipse image overlayed by the inner boundary magnetic field (sphere) and coronal magnetic field lines.

It should be noted that for the tested cases, COCONUT converged more than 30x faster than the Wind-Predict code, which is a state of art coronal model based on a regular grid with an explicit scheme [4], even though further performance-enhancement techniques such as adaptive mesh refinement or higher order reconstruction have not been implemented yet. For solar minima, our code was able to run even without any limiter applied, resulting in accuracy that was even superior that of Wind-Predict [4]. Using the same computational setup on which EUHFORIA is typically ran for space weather forecasting (6 nodes of 36 cores each on the Vlaamse Supercomputer Centre), COCONUT takes 1 to 2 hours to compute solar minima cases and 2-3 hours to compute solar maxima.

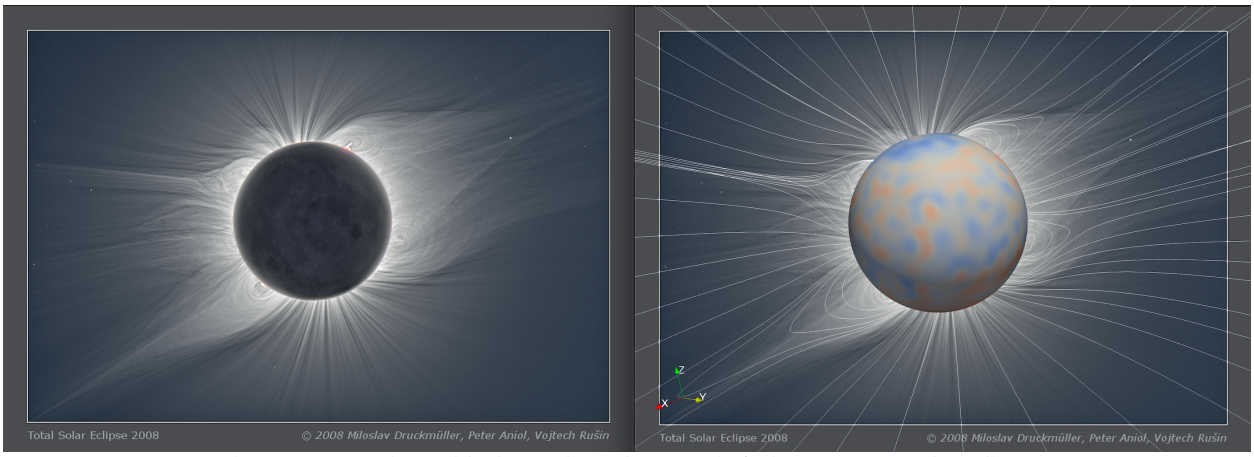

Figure 4. Comparison with observations, the case of 1st of August 2008 solar eclipse.

The reason that white light imaging has not yet been performed to evaluate the performance of the code is the fact that the simulated model is still polytropic. Inclusion of more physical terms to account for the coronal heating, radiation and conduction is currently ongoing.

SUMMARY AND CONCLUSIONS

In this paper we discussed the newly developed COCONUT global coronal model for EUHFORIA 2.0 space weather forecast. The initial studies on magnetic map reconstruction revealed that the advantage of high-l_{max} (and thus better resolved) maps is limited to the small-scale structures close to the solar surface only, while the global solution remains essentially unaffected. What is even more important, the parametric studies presented above showed that for space weather prediction purposes, maps with moderate levels of reconstruction are fully sufficient. Maps with better resolution may be crucial for studying low-corona and polar phenomena. As we focus in our work on fast-converging MHD model aimed for coupling with EUHFORIA 2.0 space weather forecast, we will use maps with reconstruction level corresponding to l_{max}=15 and l_{max}=20 in further studies. Note, that the final topology of reconstructed maps depends also on the maps source, which differs widely in resolution, min / max values and covered area of the Sun.

Our COCONUT global coronal model demonstrated a remarkable speed and accuracy over the course of testing, even in the most challenging cases of the maximum of the solar activity. As shown by the comparisons with observations, it is successful in resolving observed coronal features, while converging within operationally-feasible times, which makes it a one-of-a-kind tool potentially able to greatly improve the accuracy of our space weather forecasts with EUHFORIA 2.0. To this end, its predictions will be further improved by implementing more physical aspects, such as non-ideal terms including conduction, radiation and coronal heating. In the future, it will be also adjusted to a

multifluid formulation. Its numerical accuracy can be further improved by adaptive mesh refinement and application of higher-order flux reconstruction techniques, both of which are currently in development. Finally, the solver is currently also being developed to operate efficiently in a time-dependent fashion to allow one to simulate an insertion and evolution of flux ropes, with the aim to eventually capture the dynamics of Coronal Mass Ejections.

Acknowledgments This work has been granted by the AFOSR basic research initiative project FA9550-18-1-0093. This project has also received funding from the European Union's Horizon 2020 research and innovation program under grant agreement No. 870405 (EUHFORIA 2.0) and the ESA project "Heliospheric modelling techniques" (Contract No. 4000133080/20/NL/CRS). These results were also obtained in the framework of the projects C14/19/089 (C1 project Internal Funds KU Leuven), G.0D07.19N (FWO- Vlaanderen), SIDC Data Exploitation (ESA Prodex-12), and Belspo project B2/191/P1/SWiM. HMI data are courtesy of the Joint Science Operations Center (JSOC) Science Data Processing team at Stanford University.

REFERENCES

[1] X. Feng, *Magnetohydrodynamic Modeling of the Solar Corona and Heliosphere: Atmosphere, Earth, Ocean & Space*. Springer Nature Singapore Pte Ltd., 2020.
[2] A. R. Yeates, T. Amari, I. Contopoulos, et al., Global non-potential magnetic models of the solar corona during the March 2015 eclipse, *Space Science Reviews*, 214: 99, 2018.
[3] A. Lani, T. Quintino, D. Kimpe, el al., Reusable object-oriented solutions for numerical simulation of PDEs in a high performance environment, *Scientific Programming*, 14, 2006.
[4] B. Perri, P. Leitner, M. Brchnelova, el al., COCONUT, a novel fast-converging MHD model for solar corona simulations: I. Benchmarking and optimization of polytropic solutions, *Astrophysical Journal*, accepted, 2022.
[5] S. Poedts, A. Lani, C. Solini, et al., EUropean Heliospheric FORecasting Information Asset 2.0, *J. Space Weather Space Clim.*, 10: 57, 2020.
[6] M. Brchnelova, B. Kuźma, B. Perri, et al., To E or not to E: numerical nuances of global coronal models, *Astrophysical Journal,* accepted, 2022.
[7] Z. Yang, C. Bethge, H. Tian, et al., Global maps of the magnetic field in the solar corona, *Science,* 369: 694, 2020.
[8] A. Wagner, E. Asvestari, E. Temmer, et al.,Validation scheme for solar coronal models: constraints from multi-perspective observations in EUV and white light, *Astronomy & Astrophysics*, 657: A117, 2022.